

Effect of Screen Geometry on the Vortex Formation behind a Circular Cylinder

Open
Access

Azlin Mohd Azmi^{1,*}, Tongming Zhou²

¹ Faculty of Mechanical Engineering, Universiti Teknologi MARA, 40450 Shah Alam Selangor, Malaysia

² School of Civil, Environmental and Mining Engineering, The University of Western Australia, 35 Stirling Highway, Crawley, WA 6009, Australia

ARTICLE INFO

Article history:

Received 10 March 2018

Received in revised form 1 April 2018

Accepted 14 April 2018

Available online 16 April 2018

Keywords:

Passive control; Screen mesh; Shroud,

Vortex shedding

ABSTRACT

The wake region of a circular cylinder with and without shroud was experimentally investigated using smoke-wire flow visualization. The shrouds were made of screen cylinders, constructed from various screen meshes. The shroud-to-cylinder diameter ratio, D/d were 1.56 and 2.0 and the flow Reynolds number based on the cylinder diameter, Re_d was approximately 1000. The vortex formation process was investigated and the formation length, L_f was estimated from the flow visualization. The effect of a new dimensionless parameter, $\beta \cdot d_w/d$ (where β is the screen porosity and d_w is the mesh wire diameter) on the vortex formation length was also examined. Results showed that the formation length was greater at gap ratio of 2.0 than that at 1.6, with smaller wake width observed in the former in comparison to that in the latter. The formation length also increased with increased non-dimensional parameter $\beta \cdot d_w/d$ after its critical value was reached.

Copyright © 2018 PENERBIT AKADEMIA BARU - All rights reserved

1. Introduction

Vortex shedding and vortex-induced vibrations (VIV) has attracted strong attention from a wide range of engineering fields with one common interest of suppressing its adverse effects. As proposed by Zdravkovich [1], vortex shedding can only be delayed and weakened but never totally mitigated. Suppression of vortex shedding is achieved by modifying the flow characteristics surrounding a bluff structure to delay or control the vortex shedding; either at the boundary layer or in the wake region [2]. Historically, passive techniques have been favored because they provide cost effective solutions and are environmental compliance.

One of the passive techniques employed is a perforated shroud, an add-on device that is applied to a body or structure. The mechanism of suppression using the shrouds was first suggested by Price [3]; who hypothesized that the shroud would disrupt the flow into a large number of small vortices with the result of minimizing the periodic asymmetry of flow in the near wake. Price [3] claimed that in subcritical flow regime, the optimal shroud geometry would be that of porosity of

* Corresponding author.

E-mail address: azlinma@gmail.com (Azlin Mohd Azmi)

20-36%, diameter of $1.25d$ (where d is the diameter of the bare cylinder) and a square-hole, with holes arrangement parallel or perpendicular to the cylinder axis. Following Price's research, numerous scholars have investigated the effectiveness of various shroud designs. In particular, research into the static pressure distribution and vibrational response [4-6] found that a fine-mesh gauzed shroud, in comparison to square and circular-holed shrouds (all of 36% porosity), was most effective in reducing the vibrational double-amplitudes at high reduced velocities range, but with increased drag effect. It has also been established that perforated shrouds provide the lowest drag coefficients in comparison to other suppression devices [4, 7-9]. This is due to high base pressure and moderately secondary flow separation through the perforations. Additionally, it was found that the drag coefficient for shrouds remained fairly constant for a large range of turbulent flow conditions.

In recent years, studies of screen meshes as VIV controller have been re-examined. Azmi *et al.*, [10, 11] found that vibrational amplitude reduction of about 50% and 78% were achieved with screen shrouds of high porosity; 72% (gap ratio of 1.25) and 67% (gap ratio of 2.0), respectively. Huera-Huarte [12] studied meshes of two different hole sizes ($0.1d$ and $0.36d$) at various gap ratio from 0.5 to 1.3 and showed that more than 95% suppression of VIV was attained for reduced velocities up to more than 13, with drag reductions of 20% inside the lock-in region, proving the advantages of the screen shroud as suppression device.

The wake characteristics of a single screen cylinder were also studied by several researchers. Takeuchi *et al.*, [13] showed that the reattachment point behind their permeable cylinders made of wire mesh of 54% and 71% porosities was delayed several times of that a solid cylinder wake. In contrast, Gansel *et al.*, [14] revealed that at porosity just below 75%, the wake characteristics behind their metal meshed cylinders (at Reynolds numbers ranging from 1000-20,000) changed toward that of a solid cylinder. A later study by Levy *et al.*, [15] proposed an empirical parameter based on the twine to mesh ratio which was more appropriate in defining the flow topology through a porous cylinder for $Re < 800$, rather than porosity alone.

Despite findings from the above literatures, the effect of screen geometries (other than porosity) on the wake dynamics was not explored fully and our understanding is still incomplete. Evidently, flow past a screen shrouded cylinder cannot be predicted solely on porosity since there are numerous length scales involved such as circular cylinder diameter, shroud diameter, screen wire diameter and screen aperture (hole size). A preliminary study has been conducted in understanding the effect of the screen parameters on the circular cylinder wake and can be found from [16]. The present study aims to provide additional insight into these parameters to understand their influence in suppressing vortex shedding from a circular cylinder.

2. Dimensional Analysis

A dimensional analysis was performed using method of repeating variables to generate the non-dimensional parameters influencing the flow behind the cylinders. We know that the vortex formation length, L_f is a function of parameters given below

$$L_f = f(\rho, \mu, U_\infty, d, D, d_w, \alpha) \quad (1)$$

where ρ is the fluid density, μ is the fluid kinematic viscosity, U_∞ is the free stream velocity, d is the diameter of a plain circular cylinder, D is the diameter of the shroud, d_w is the diameter of the mesh wire, and α is the mesh hole size. Using independent scaling variables of ρ , U_∞ and d , the above equation reduces to a non-dimensional form given below,

$$L_f/d = f(Re_d, D/d, d_w/d, a/d) \quad (2)$$

where Re_d is the Reynolds number based on the plain circular cylinder diameter, D/d corresponds to the gap ratio, d_w/d is the screen mesh wire-to-plain cylinder diameter ratio and a/d is the aperture-to-diameter of plain cylinder ratio. It is obvious that the flow field is highly influenced by these parameters. Hence, the present study is with reference to these parameters, keeping the Reynolds number fix. The gap ratio effect is studied at 1.56 and 2.0. Since the screens were in predetermined configurations from the manufacturer (Locker Group), the two remaining screen parameters (d_w and a) vary according to porosity; i.e. for screens with the same mesh wire diameter, porosity will be different depending on the hole size and vice versa. Knowing porosity a function of hole size and wire diameter, i.e. $\beta = a^2 / (a + d_w)^2$, the non-dimensional parameters are manipulated to form a new parameter of $\beta \cdot d_w/d$, combining both the geometries of the screen and the plain circular cylinder while reducing the number of necessary independent parameters.

3. Experimental Details

The experiments were conducted in a small open circuit type wind tunnel with a test section of 380 mm (width) x 255 mm (height) and 1.8 m (long). The free stream velocity in the test section was uniform to 0.2%, and the longitudinal turbulence intensity was less than 0.5%. Experiments were conducted in the wakes of both the circular cylinder and shrouded cylinders. For the plain cylinder experiment, a circular cylinder made of polished aluminium with diameter d of 25 mm were used. Screen cylinders, rolled from various stainless steel wire meshes of square cross sections were used as shrouds (named as Screen 1-4). The screen cylinders were made in accordance to [17]. The diameter of the screen shrouds, D was 25 mm. The same shrouds were attached to different circular cylinders of diameter of 12.7 mm and 16 mm, giving a shroud-to-cylinder diameter gap ratio, D/d of about 2.0 and 1.56, respectively. The properties of the screen meshes are given in Table 1. Both the plain circular cylinder and the shrouded cylinders aspect ratio, l/d (or l/D) were 15.2. Figure 1 shows the shrouded cylinder set up and one of the screen cylinders used in the study.

Table 1
 Properties of screen meshes

Screen	Hole Size, a (mm)	Wire Diameter, d_w (mm)	Porosity, β (%)	Dimensionless parameter, $\beta d_w/d$ at $D/d=1.56$	Dimensionless parameter, $\beta d_w/d$ at $D/d=2.0$	Formation length, L_f/d at $D/d=1.56$	Formation length, L_f/d at $D/d=2.0$
1	0.25	0.16	37	0.47	0.37	9	16
2	0.71	0.32	48	1.21	0.96	9	16
3	1.6	0.45	61	2.16	1.72	19	31
4	2	0.45	67	2.37	1.88	25	39

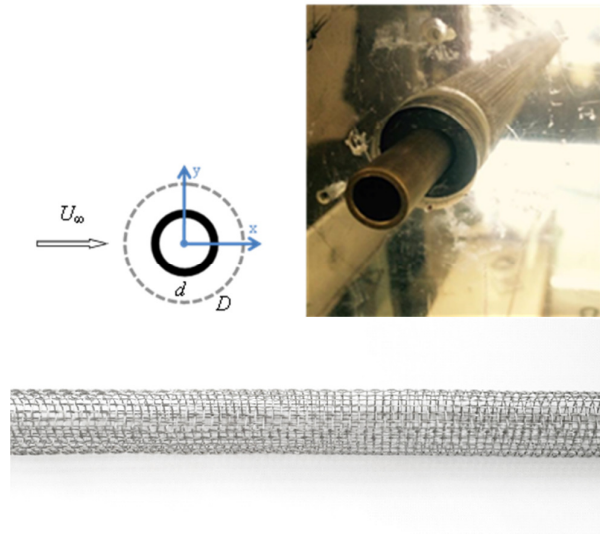


Fig. 1. Shrouded cylinder set up and one of the screen cylinders used in the experiment.

Smoke wire flow visualizations were carried out using a high speed camera to obtain a qualitative understanding on the vortex formation process. Smoke was produced from a thin (0.1 mm) nickle wire coated with oil. The wire was connected as a resistor to an electric circuit. When voltage was applied to the wire, the heat of the wire caused the oil to evaporate, creating short bursts of smoke filaments which was carried downstream by the flow to reveal the flow motion. The visualizations were conducted at Reynolds numbers (based on the circular cylinder diameter) of approximately 1000.

4. Results and Discussion

Figure 2 shows the vortex formation behind a plain circular cylinder. Large-scale vortices are shed alternately into the wake, forming a von Kármán vortex street. The two rows of counter-rotating vortex structures are connected by the streamwise rib-like structures that are stretched due to the counter-rotating vortices. The vortices interact with each other, penetrating to the opposite side across the wake centreline when evolving downstream. The formation length of the Kármán vortices is about $2d$ which is in good agreement with [18]. Note that the formation length is scaled by D in all subsequent figures for visualization purpose but results summary will be reported based on d .

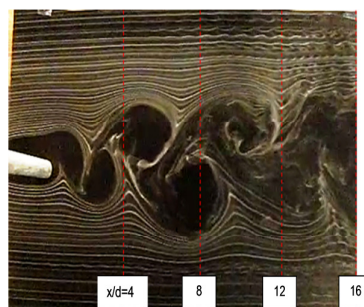


Fig. 2. Vortex formation in a circular cylinder wake

Figures 3 to 6 illustrate the influence of the screen shrouds on the wake of a circular cylinder. There is an onset of transition in the shear layers and the development of turbulence in the wake further downstream, similar to that in the circular cylinder wake but the formation length is delayed significantly. While vortex is being drawn across the wake of a circular cylinder, this seems not so evident with the inclusion of the screen shrouds. Figure 3 shows that with screen 1, the onset of shear layer interaction occurs at approximately $6D$ (or $9d$) and $8D$ (or $16d$) at gap ratios of 1.56 and 2.0, respectively. An undulation of the shear layers are evident, followed by the formation of the large-scale structures. The size of these structures is bigger (resulting in a wider wake) at gap ratio of 1.56 in comparison to that at 2.0. With screen 2 (Fig. 4), the wake behavior is also similar to that observed with screen 1 (Fig. 3). It seems that at both gap ratios of 1.56 and 2.0, the formation length in the cylinder wake with screen 1 are at the same range of that with screen 2.

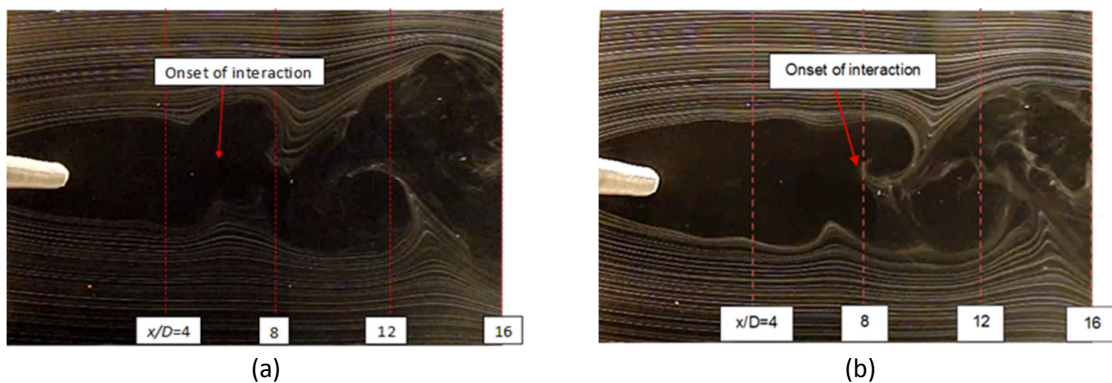


Fig. 3. Vortex formation in a screen shrouded cylinder wake using screen 1 at gap ratio of a) 1.56 and b) 2.0

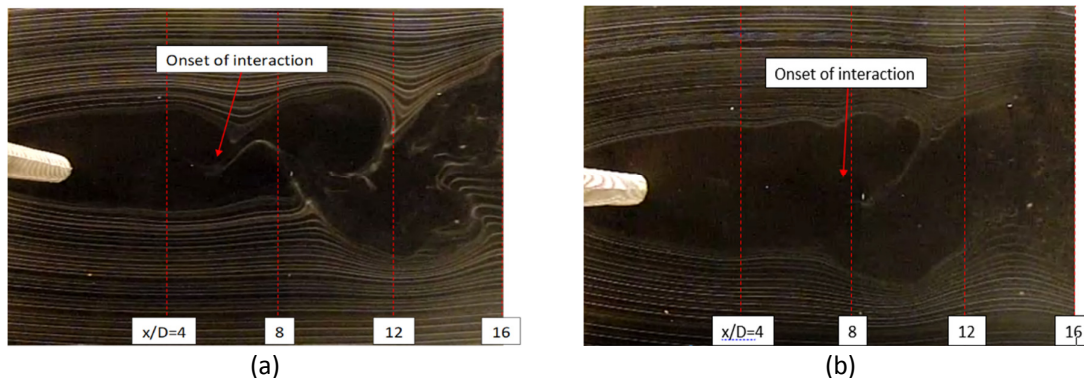


Fig. 4. Vortex formation in a screen shrouded cylinder wake using screen 2 at gap ratio of a) 1.56 and b) 2.0

Figure 5 and 6 shows clearly the formation of small-scale vortices prior to the large ones and the formation length is delayed greatly in comparison to the previous two cases. The wake widths in these regions are also small. These small-scale vortices grow downstream gradually before rolling up to form the large-scale structures through amalgamation of several vortices which is apparent from Figure 5. These large-scale structures only start to form at about $x/D \geq 12$. With screen 4 (Fig.

6), it is observed that the formation occurs at about $x/D = 16$ and 20 , respectively (not shown), extending enormously the formation length.

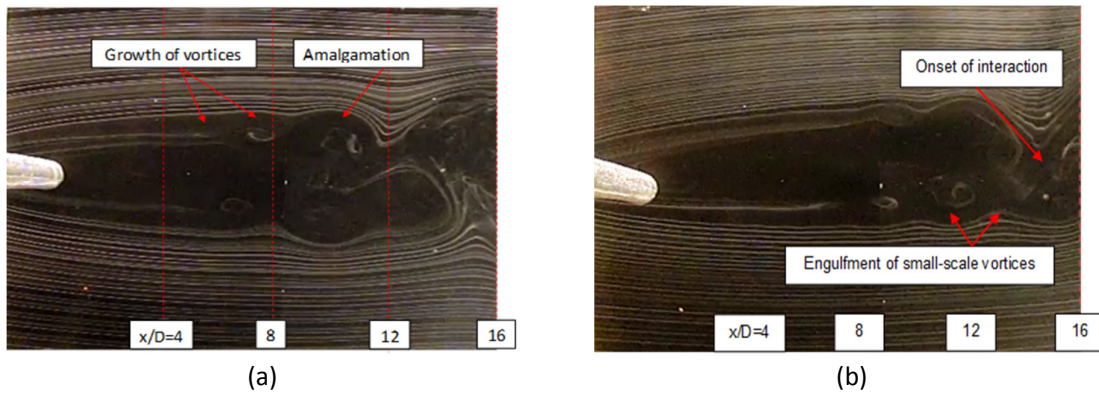


Fig. 5. Vortex formation in a screen shrouded cylinder wake using screen 3 at gap ratio of a) 1.56 and b) 2.0

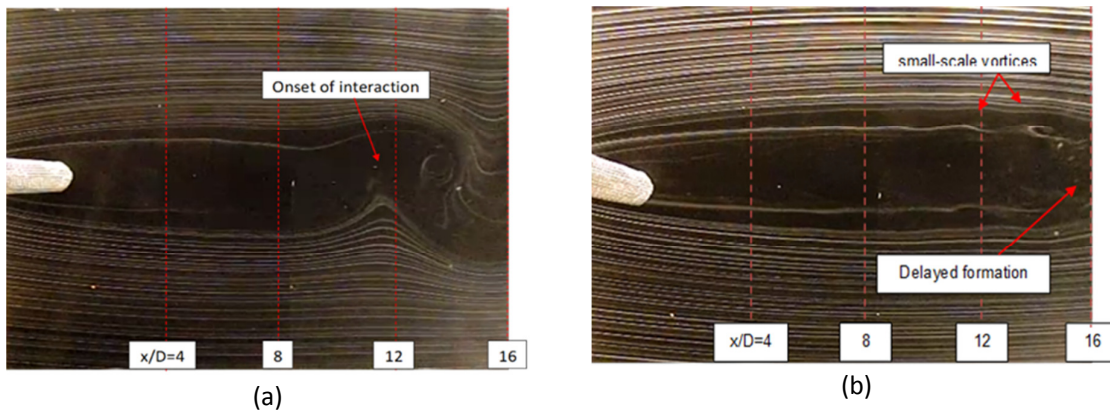


Fig. 6. Vortex formation in a screen shrouded cylinder wake using screen 4 at gap ratio of a) 1.56 and b) 2.0

Table 1 summarizes the formation length L_f/d for different screen parameters and the result is presented in Figure 7. Figure 7 indicates that the non-dimensional parameter has fair influence on the vortex formation length. As $\beta \cdot d_w/d$ increases, the formation length increases exponentially, with greater influence at gap ratio 2.0 than that at 1.56. There seems to be a critical value where the formation length lies around a similar range at respective gap ratio, i.e. about $\beta \cdot d_w/d < 1.0$ at gap ratio of 1.56 and $\beta \cdot d_w/d < 1.5$ at gap ratio of 2.0. This needs to be explored and corroborated with more testing on various screen meshes.

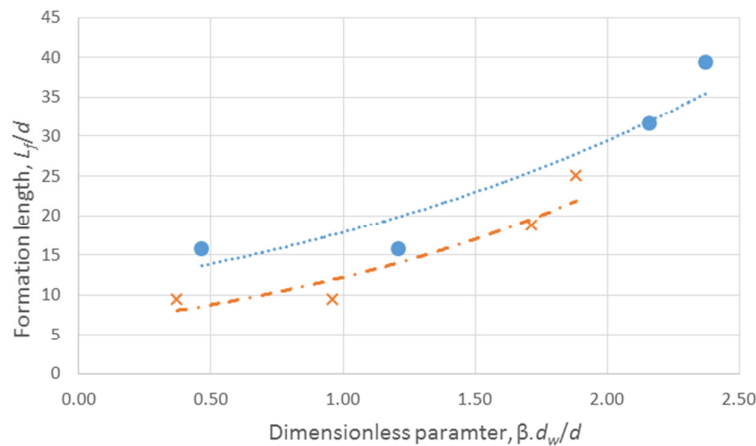


Fig. 7. Relationship between the dimensionless parameters and formation length

5. Conclusions

The flow visualization has provided insight into the vortex formation process and the influence of screen geometry behind a circular cylinder. The presence of the screen shrouds significantly extended the vortex formation length with longer formation length and smaller wake width perceived at gap ratio of 2.0 than that at 1.5. The formation length also increased with the non-dimensional parameter, $\beta.d_w/d$, after reaching some critical values. It was also evident that the vortex formation in the screen shrouded cylinder wakes were characterized by the evolution of the small-scale vortices that grew bigger downstream through vortex merging, coupled with the interaction of the two shear layers. Future studies should include a great variety of screen meshes to really understand the effect of the screen parameters on the wake behind a circular cylinder.

Acknowledgement

This research was funded by a grant from Universiti Teknologi MARA (600-IRMI/MyRA 5/3/LESTARI (0049/2016)).

References

- [1] Zdravkovich, M. M. "Review and classification of various aerodynamic and hydrodynamic means for suppressing vortex shedding." *Journal of Wind Engineering and Industrial Aerodynamics* 7, no. 2 (1981): 145-189.
- [2] Choi, Haecheon, Woo-Pyung Jeon, and Jinsung Kim. "Control of flow over a bluff body." *Annu. Rev. Fluid Mech.* 40 (2008): 113-139.
- [3] Price, Peter. "Suppression of the fluid-induced vibration of circular cylinders." *Journal of the Engineering Mechanics Division* 82, no. 3 (1956): 1-22.
- [4] Wong, H. Y. "A means of controlling bluff body flow separation." *Journal of Wind Engineering and Industrial Aerodynamics* 4, no. 2 (1979): 183-201.
- [5] Zdravkovich, M. M. "Circular cylinder enclosed in various shrouds." ASME, 1971.
- [6] Zdravkovich, M. M., and J. R. Volk. "Effect of shroud geometry on the pressure distributed around a circular cylinder." *Journal of Sound and Vibration* 20, no. 4 (1972): 451-455.
- [7] Knell, B. J. "The drag of a circular cylinder fitted with shrouds." *NPL Aero Report* 1297 (1969).
- [8] Wong, H. Y., and A. Kokkalis. "A comparative study of three aerodynamic devices for suppressing vortex-induced oscillation." *Journal of Wind Engineering and Industrial Aerodynamics* 10, no. 1 (1982): 21-29.
- [9] Wootton, L. R., and D. Yates. "Further experiments on the drag of circular cylinders fitted with various shrouds." *NPL Aero Report* 1321 (1970).

- [10] Azmi, Azlin Mohd, Tongming Zhou, Yu Zhou, Jianggang Chen, and Liang Cheng. "The effect of a screen shroud on vortex-induced vibration of a circular cylinder and its wake characteristics." In *The Twenty-fifth International Ocean and Polar Engineering Conference*. International Society of Offshore and Polar Engineers, 2015.
- [11] Azmi, Azlin Mohd, Tongming Zhou, Liang Cheng, Hanfeng Wang, and Leok Poh Chua. "On the effectiveness and mechanism of vortex-induced vibration suppression using a screen cylinder." In *The Twenty-second International Offshore and Polar Engineering Conference*. International Society of Offshore and Polar Engineers, 2012.
- [12] Huera-Huarte, F. J. "Suppression of vortex-induced vibration in low mass-damping circular cylinders using wire meshes." *Marine Structures* 55 (2017): 200-213.
- [13] Takeuchi, Hirotsuka, Yuji Tasaka, Yuichi Murai, Yasushi Takeda, Hideaki Tezuka, and Michitsugu Mori. "Particle image velocimetry for air flows behind permeable cylinders." In *ASME/JSME 2007 5th Joint Fluids Engineering Conference*, pp. 671-678. American Society of Mechanical Engineers, 2007.
- [14] Gansel, Lars C., Thomas A. McClimans, and Dag Myrhaug. "The effects of fish cages on ambient currents." *Journal of Offshore Mechanics and Arctic Engineering* 134, no. 1 (2012): 011303.
- [15] Levy, B., Heide Friedrich, J. E. Cater, R. J. Clarke, and J. P. Denier. "The impact of twine/mesh ratio on the flow dynamics through a porous cylinder." *Experiments in fluids* 55, no. 10 (2014): 1829.
- [16] Azmi, A. M., and T. Zhou. "Passive Control of Vortex Shedding via Screen Shroud." In *IOP Conference Series: Materials Science and Engineering*, vol. 280, no. 1, p. 012028. IOP Publishing, 2017.
- [17] Azmi, Azlin Mohd, Tongming Zhou, Yu Zhou, and Liang Cheng. "Statistical analyses of a screen cylinder wake." *Fluid Dynamics Research* 49, no. 1 (2016): 015506.
- [18] Unal, M. F., and D. Rockwell. "On vortex formation from a cylinder. Part 1. The initial instability." *Journal of Fluid Mechanics* 190 (1988): 491-512.